

Automatic Termination Strategy of Inelastic Neutron-scattering Measurement Using Bayesian Optimization for Bin-width Selection

Kensuke Muto^{1,4}, Hirotaka Sakamoto¹, Kenji Nagata², Taka-hisa Arima³, and Masato Okada^{2,3*}

¹*Graduate School of Frontier Sciences, The University of Tokyo, Chiba 277–0882, Japan*

²*Research and Services Division of Materials Data and Integrated System, National Institute for Materials Science, Tsukuba, Ibaraki 305–0047, Japan*

³*Graduate School of Frontier Sciences, The University of Tokyo, Chiba 277–8561, Japan*

⁴*Karakuri, Inc., 2-7-3 Tsukiji, Chuo-ku, Tokyo 104-0045, Japan*

Currently, an excessive amount of event data is being obtained in four-dimensional inelastic neutron-scattering experiments. A method for automatic bin-width optimization of multidimensional histograms has been developed and recently validated on real inelastic neutron-scattering data. However, measuring beyond the equipment resolution leads to inefficient use of valuable beam time. To improve experimental efficiency, an automatic termination strategy is essential. We propose a Bayesian-optimization-based method to compute stopping criteria and determine whether to continue or terminate the experiment in real time. In the proposed method, the bin-width optimization is performed using Bayesian optimization to efficiently compute the optimal bin widths. The experiment is terminated when the optimal bin widths become smaller than the target resolutions. In numerical experiments using real inelastic neutron-scattering data, the optimal bin widths decrease as the number of events increases. Even the optimal bin widths for data downsampled to 1/5 are comparable with the resolutions limited by the sample size, choppers, and so on. This implies excessive measurement of the inelastic neutron experiments for the moment. Moreover, we found that Bayesian optimization can reduce the search cost to approximately 10% of an exhaustive search in our numerical experiments.

*okada@edu.k.u-tokyo.ac.jp

1. Introduction

Inelastic neutron-scattering is an experimental method for investigating the dynamical structure of materials.¹⁾ In recent years, numerous event data have been obtained in inelastic neutron-scattering experiments using high-power accelerator-based neutron sources such as those of ISIS,²⁾ SNS,³⁾ J-PARC,⁴⁾ and CSNS.⁵⁾ A time-of-flight neutron spectrometer designed for inelastic scattering measurements, such as MAPS,⁶⁾ MERLIN,⁷⁾ HYSPEC,⁸⁾ ARCS,⁹⁾ 4SEASONS,¹⁰⁾ AMATERAS,¹¹⁾ and HRC,¹²⁾ produces a large-scale event data. Researchers obtain event data mapped on the four-dimensional (4D) space of transferred energy (E) and momentum (\mathbf{q}). At present, researchers create histograms from the obtained event data and analyze them.¹³⁾ It is necessary to set the bin widths when creating a histogram.

Shimazaki and Shinomoto proposed a one-dimensional histogram bin-width optimization method based on minimizing a cost function, originally developed for neuronal spike trains in neuroscience.¹⁴⁾ They also proposed an extrapolation theory to predict how optimal bin width changes as the number of trials increases. This extrapolation theory provides a practical way to estimate how many additional experimental trials are needed to construct a meaningful histogram with sufficient resolution. Muto et al. extended this approach to multidimensional histograms by using summed-area tables (SAT).^{15,16)} The SAT implementation substantially reduces the computational cost of evaluating the cost function for multidimensional histograms. Recently, Tatsumi et al. applied this bin-width optimization method to real inelastic neutron-scattering data and validated both the optimization method and the extrapolation theory for Cu single crystal measurements at J-PARC.¹⁷⁾

A practical application of multidimensional bin-width optimization is to determine whether to stop or to continue the experiment. By using a larger amount of data, we can extract more detailed features of the target materials. However, measuring beyond the resolution of the measurement equipment leads to inefficient use of valuable beam time. While the extrapolation theory predicts how optimal bin widths change with data size, it cannot exactly predict the optimal bin widths for each specific measurement; thus, accurate stopping decisions require real-time bin-width optimization during the experiment. Tatsumi et al. demonstrated that parallel computation on a 32-core Xeon processor enabled such real-time optimization.¹⁷⁾ However, parallel computation infrastructure requires significant operational resources. We propose a Bayesian-optimization-based method to compute the stopping criteria and determine whether to stop or continue the experiment in real time. The flowchart of the method is shown in Fig. 1. By using Bayesian optimization to efficiently search for

optimal bin widths, our approach achieves real-time performance without requiring parallel-computation infrastructure. The experiment is terminated when the optimal bin widths become smaller than the expected resolutions. We conducted numerical experiments using real experimental data and found that the optimal bin widths decrease as the number of data increases, which is consistent with previous studies.^{14,15,17)} Moreover, we found that Bayesian optimization can reduce the search cost to approximately 10% of exhaustive search in our numerical experiments. This computational efficiency demonstrates that our approach can serve as a practical stopping criterion for routine inelastic neutron-scattering experiments.

The structure of this paper is as follows. In Section 2, we formulate a method of multidimensional bin-width optimization and Bayesian optimization. In Section 3, we present the numerical experiments using some real experimental data to explain the significance of studying a stopping strategy and efficiency of Bayesian optimization. We discuss the results in Section 4 and provide conclusions in Section 5.

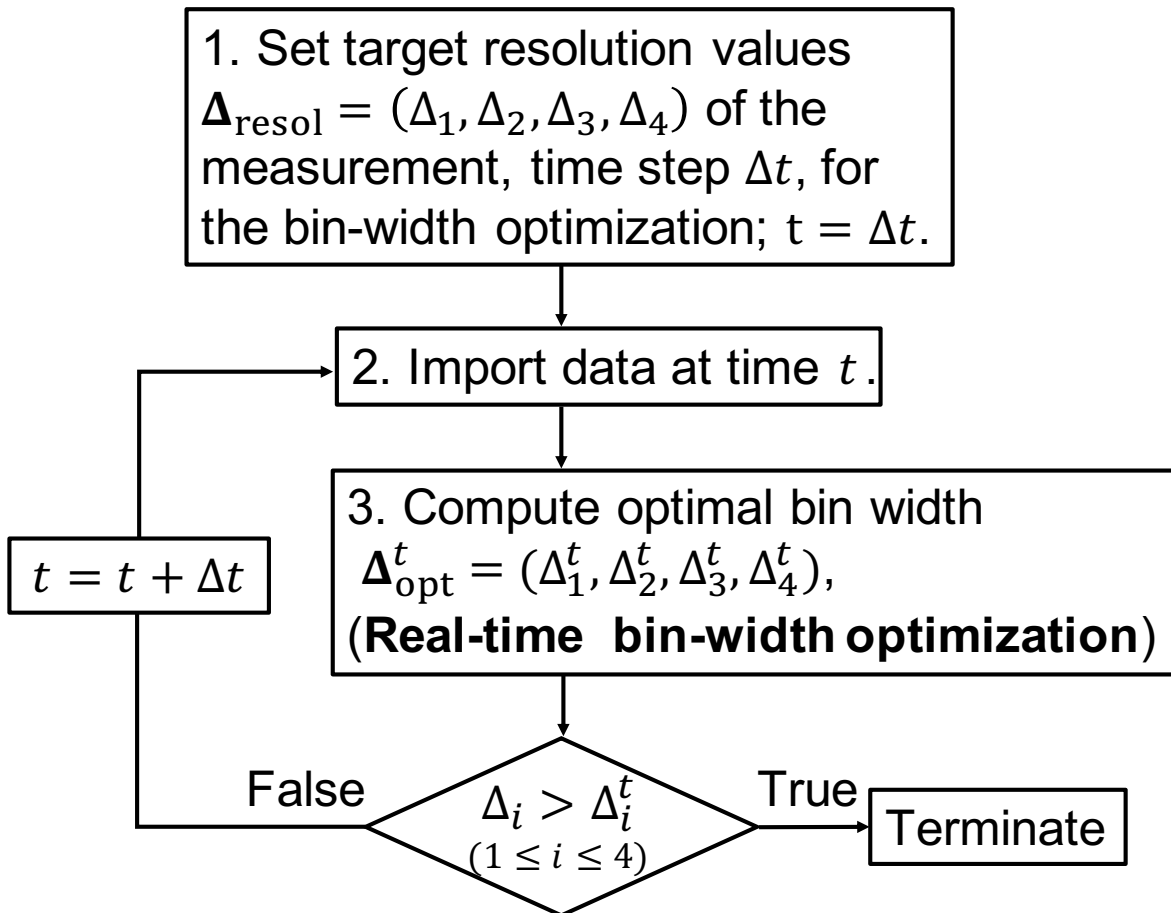


Fig. 1. Overview of the termination strategy.

2. Method

2.1 Bin-width optimization for one-dimensional event data

Shimazaki and Shinomoto proposed a bin-width optimization method for 1D data.¹⁴⁾ They considered a case where researchers obtain n pieces of event data $t_i \in [0, T]$ ($1 \leq i \leq n$) in the observation time interval $[0, T]$ and the data follow a true probability density $\lambda(t)$. The performance of the estimator $\hat{\lambda}(t)$ for $\lambda(t)$ can be evaluated using the mean integrated squared error (MISE) as follows,

$$\text{MISE} = \frac{1}{T} \int_0^T E \left[(\hat{\lambda}(t) - \lambda(t))^2 \right] dt. \quad (1)$$

In statistics, MISE is used for density estimations.¹⁸⁾ Here, $E[\cdot]$ represents the expectation over different realizations of event data given by $\lambda(t)$. When the observation interval is equally divided into N parts, the estimator $\hat{\lambda}(t)$ is limited to the form of the histogram of the bin width $\Delta = \frac{T}{N}$. A cost function is derived by extracting the terms depending on the bin width Δ from the right side of Eq. (1), as

$$\hat{C}(\Delta) = \frac{2\bar{k} - v}{\Delta^2}, \quad (2)$$

$$\text{where } \bar{k} = \frac{n}{N}, v = \frac{1}{N} \sum_{i=1}^N (k_i - \bar{k})^2. \quad (3)$$

Here, k_i represents the number of events contained in the i -th bin. We define the optimal bin width as the bin width that minimizes the cost function.

2.2 Multidimensionalization of the bin-width optimization algorithm

We will consider a case where researchers obtain n pieces of event data mapped on \mathbb{R}^d . To make a histogram, we divide the observation area equally into N d -dimensional rectangular parallelepipeds with bin widths $\Delta_1, \Delta_2, \dots, \Delta_d$. Similarly to the 1D case, we can compute the cost function $\hat{C}_n(\Delta_1, \Delta_2, \dots, \Delta_d)$ as

$$\hat{C}(\Delta_1, \Delta_2, \dots, \Delta_d) = \frac{2\bar{k} - v}{(\Delta_1 \Delta_2 \dots \Delta_d)^2}, \quad (4)$$

$$\text{where } \bar{k} = \frac{n}{N}, v = \frac{1}{N} \sum_{i=1}^N (k_i - \bar{k})^2, \quad (5)$$

where k_i represents the number of events contained in the i -th bin. The estimator of the height of the i -th bin is $\hat{\theta}_i = \frac{k_i}{n \Delta_1 \Delta_2 \dots \Delta_d}$. Moreover, in the multidimensional case, optimal bin widths minimize the cost function.

The computational cost of calculating the optimal bin widths increases as the dimension d increases, and therefore it is essential to reduce the cost. Using the summed-area table (SAT)

algorithm, as shown in Fig. 2 for $d = 2$, we can reduce the computational complexity for the number of counts in each bin.¹⁶⁾ To apply the SAT algorithm, it is necessary to obtain event data in a sufficiently fine histogram. The steps of SAT are shown in Algorithm 1. Since it is

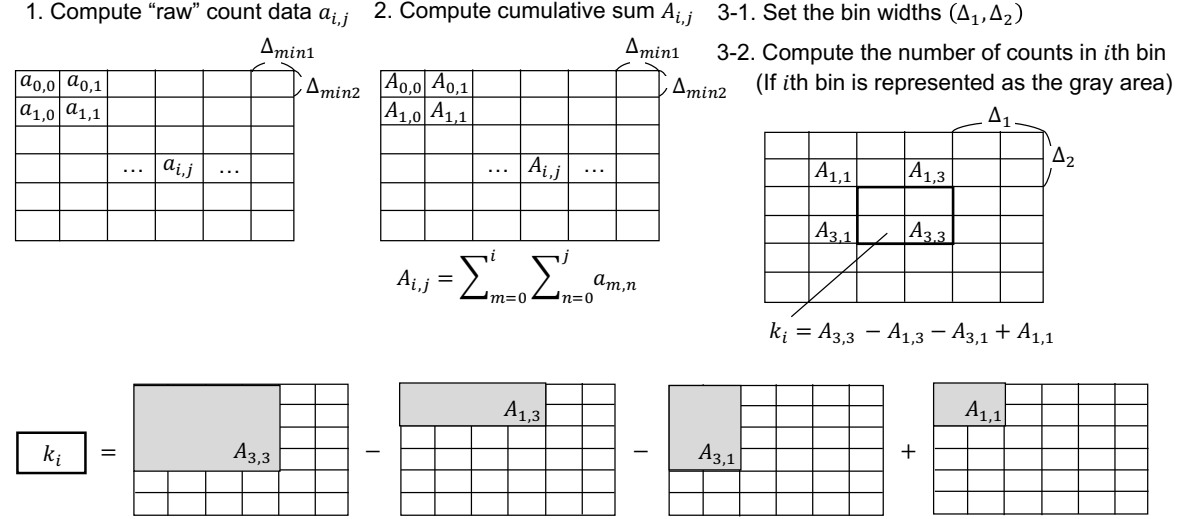


Fig. 2. Overview of the summed-area tables algorithm for the 2D case. We set a sufficient fine histogram and call it "raw" count data $a_{i,j}$.

not necessary for the termination strategy to find the exact optimal bin widths, we consider only multiples of the minimum units of bin widths. It is sufficient to set the maximum value of Δ_i to being several times as large as the required resolution.

Let us discuss the computational complexity of the bin-width optimization. Denote the maximum division number in the i -th dimension as $N_{max,i}$. Let N_i be the number of axial divisions in the i -th dimension, and consider the case where the cost function is computed by setting N_i from 2 to $N_{max,i}$. Then, the computational cost of the bin-width optimization is $O(\prod_{i=1}^d N_{max,i} \log N_{max,i})$.

2.3 Bayesian optimization

Bayesian optimization is a method for solving optimization problems involving an objective function. Moreover, a Gaussian process (GP) is often used to interpolate the objective function by using correlation based on the distance between the observation points. Bayesian optimization uses the results of the interpolation to select the next point to maximize the acquisition function. Here, we treat the expected improvement (EI)¹⁹⁾ as the acquisition func-

Algorithm 1 Bin-width optimization (multidimensional case)

Step 1:

Set the minimum units of the bin widths: $\Delta_{min,1}, \Delta_{min,2}, \dots, \Delta_{min,d}$ and compute “raw” count data as shown in Fig. 2(a). Compute the cumulative sum A_{i_1, i_2, \dots, i_d} of the “raw” count data for preparation of the SAT algorithm.

Step 2:

Set the bin widths $(\Delta_1, \Delta_2, \dots, \Delta_d)$. Compute the number of counts k_i in the i -th bin by using the SAT algorithm. Then, compute ν defined in Eq. (5). Compute $\hat{C}(\Delta)$ defined in Eq. (4).

Step 3:

Repeat step 2 to find the bin width Δ that minimizes $\hat{C}(\Delta)$, and let this be the optimal bin width.

tion:

$$EI(\mathbf{x}) = \begin{cases} (f^* - \mu(\mathbf{x}))\Phi\left(\frac{f^* - \mu(\mathbf{x})}{\sigma(\mathbf{x})}\right) + \sigma(\mathbf{x})\phi\left(\frac{f^* - \mu(\mathbf{x})}{\sigma(\mathbf{x})}\right), & (\sigma(\mathbf{x}) > 0) \\ 0. & (\sigma(\mathbf{x}) = 0) \end{cases} \quad (6)$$

$\mu(\mathbf{x})$ and $\sigma(\mathbf{x})$ are the mean and variance functions of the Gaussian process at point \mathbf{x} , respectively, and f^* is the minimum value among the observed data. ϕ and Φ represent the normalized Gaussian function and its cumulative distribution function. EI has been proven to have convergence properties.²⁰⁾ The computational complexity of the acquisition function is $O(N^2)$ when the hyperparameter (HP) of GP is fixed, and $O(N^3)$ when the HP of GP is tuned sequentially. Here, N represents the number of searched points.

3. Results

We performed numerical experiments with experimental data to verify the validity of the proposed method. The data consisted of inelastic neutron-scattering measurements on $\text{Ba}_3\text{Fe}_2\text{O}_5\text{Cl}_2$. The unit cell of this material is body-centered cubic with a lattice constant of 9.96\AA .²¹⁾ First, we computed the cost function for the whole experimental data and found the optimal bin widths. Then, we conducted downsampling to vary the number of events and computed the cost function for each downsampled data. Then, we examined the relationship between the number of events and the optimal bin widths. Finally, we examined the effectiveness of BO in finding the optimal bin widths. The resolution of the experimental equipment was $\Delta_{\text{resol}} = (5, 0.25, 0.25, 0.30)[\text{meV}, \text{r.l.u.}, \text{r.l.u.}, \text{r.l.u.}]$.

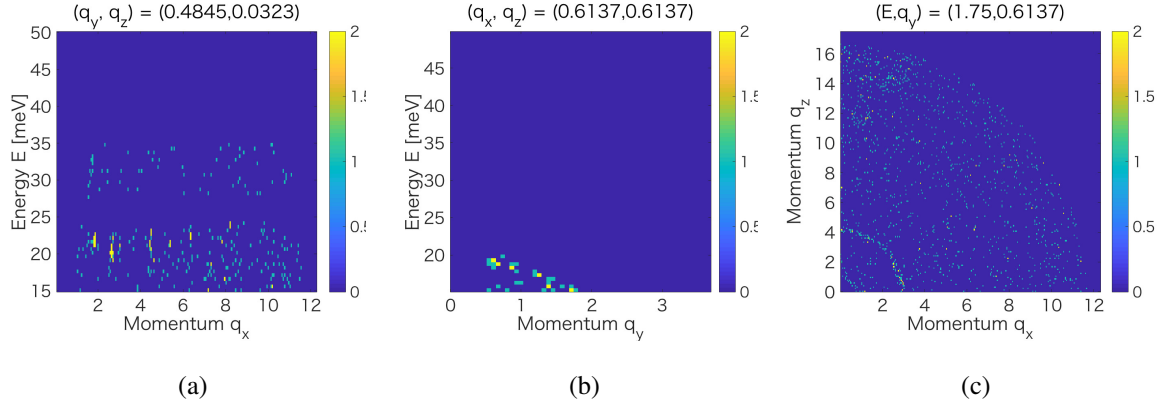


Fig. 3. 2D slices of 4D inelastic neutron-scattering count data. Regarding (a), q_y and q_z are fixed at 0.4845 ± 0.0323 and 0.0323 ± 0.0323 , respectively. Regarding (b), q_x and q_z are fixed at 0.6137 ± 0.0323 and 0.6137 ± 0.0323 , respectively. Regarding (c), E and q_y are fixed at 1.75 ± 0.25 and 0.6137 ± 0.0323 , respectively. The upper bound of the color axes is set to 2.

3.1 Bin-width optimization for experimental data

We experimented with inelastic neutron-scattering data within $15 [\text{meV}] \leq E \leq 50 [\text{meV}]$ and momentum components $0 \leq q_x, q_y, q_z$, in which there were 1,679,542 events. To use the SAT algorithm, we set the minimum units of the bin widths in the energy and momentum directions as $\Delta_{\min,E} = 0.5 [\text{meV}]$ and $\Delta_{\min,q} = 0.13 [\text{r.l.u.}]$, respectively. We limited the search area for the optimal bin widths to multiples of the minimum unit. Since we do not consider the case where the number of events is extremely small, we limit the search space of the bin width up to 10 times the minimum unit in each dimension. Since we considered a 4D space, there were a total of 10,000 search candidates. To simulate the process of increasing data while conducting a measurement, we generated data downsampled at a rate of r_{ds} from the full data. We computed the cost functions for $r_{ds} = 0.1, 0.2, 0.5, 1$. Fig. 3 shows 2D slices of the 4D data. To visualize the relation between the number of events and the optimal bin widths, we plotted the one-dimensional profile of the cost functions (Fig. 4). To unify the scale of the cost functions for different data sizes, we divided each cost function by the square of the number of events. The optimal bin widths $(\Delta_E, \Delta_{q_x}, \Delta_{q_y}, \Delta_{q_z})$ [meV, r.l.u., r.l.u., r.l.u.] were $(4, 0.32, 0.26, 0.32)$, $(4, 0.19, 0.13, 0.32)$, $(3, 0.13, 0.13, 0.19)$, and $(2, 0.13, 0.13, 0.13)$ for $r_{ds} = 0.1, 0.2, 0.5$, and 1, respectively. The optimal energy bin width for $r_{ds} = 0.1$ was smaller than the energy resolution of the experiment $\Delta_{\text{resol},E}$.

3.2 Searching for the optimal bin width by using Bayesian optimization

We carried out numerical experiments to verify the efficiency of BO in searching for optimal bin widths in which we applied BO to the cost functions for the downsampled data.

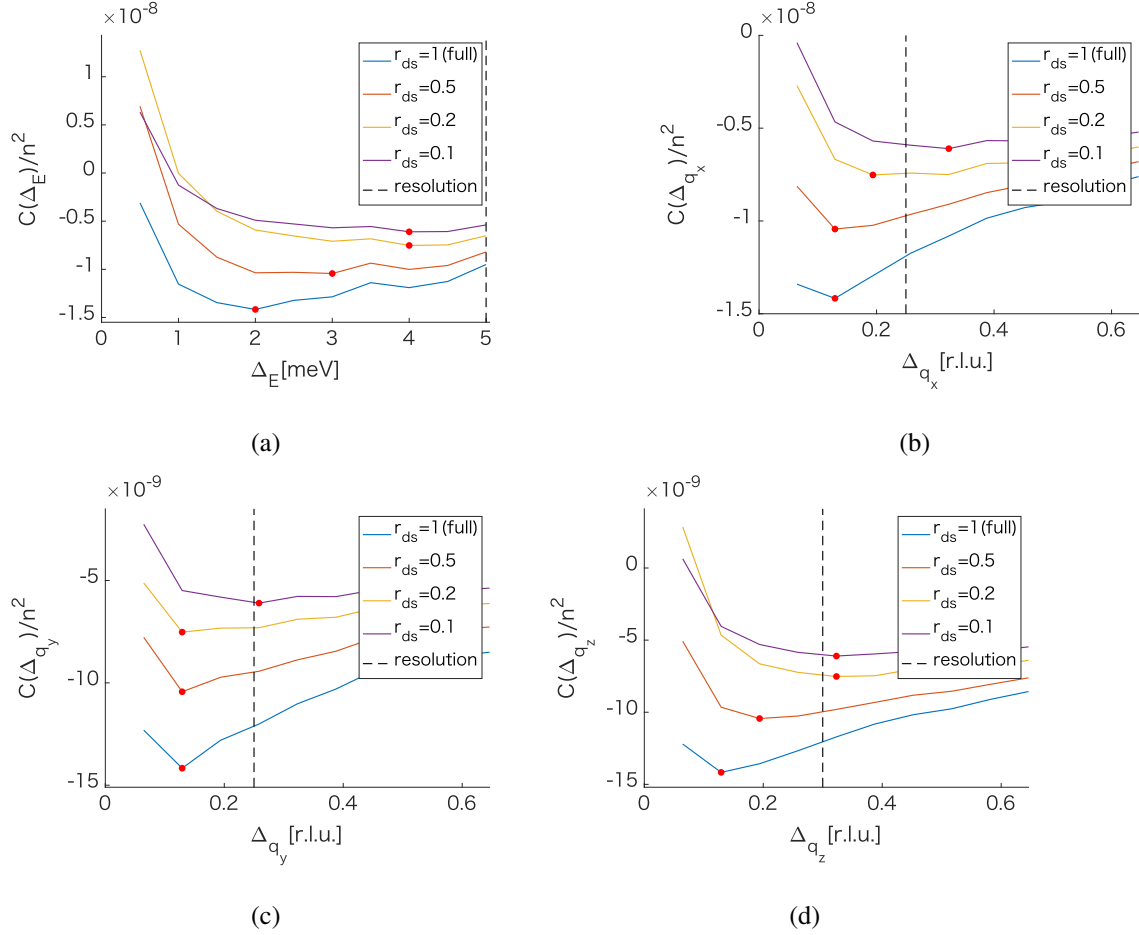


Fig. 4. 1D slices of 4D cost functions computed by changing the downsampling rate of r_{ds} . To unify the scale, each cost function is divided by the square of the number of events. (a)–(d) represent landscapes of the cost functions in the E , q_x , q_y , and q_z direction. The cost value in one axis direction is visualized, and the other three axis directions are fixed to the optimal bin width. The optimal bin widths ($\Delta_E, \Delta_{q_x}, \Delta_{q_y}, \Delta_{q_z}$) are (4[meV], 0.32, 0.26, 0.32) for $r_{ds} = 0.1$, (4[meV], 0.19, 0.13, 0.32) for $r_{ds} = 0.2$, (3[meV], 0.13, 0.13, 0.19) for $r_{ds} = 0.5$, and (2[meV], 0.13, 0.13, 0.13) for $r_{ds} = 1$. Approximate optimal bin widths and the experiment’s resolutions are represented as filled circles and dashed lines.

We performed 100 experiments for each r_{ds} with different initial ($\Delta_E, \Delta_{q_x}, \Delta_{q_y}, \Delta_{q_z}$) points. We used MATLAB’s `bayesopt` function and set the acquisition function to EI+. The results of the numerical experiments are visualized in Fig. 5. Moreover, we estimated the computational complexity of the BO search and compared its computational cost with that of the 10,000 point search. For estimating the computational cost, we computed the sum of the number of divisions for each Δ . The results are shown in Fig. 6.

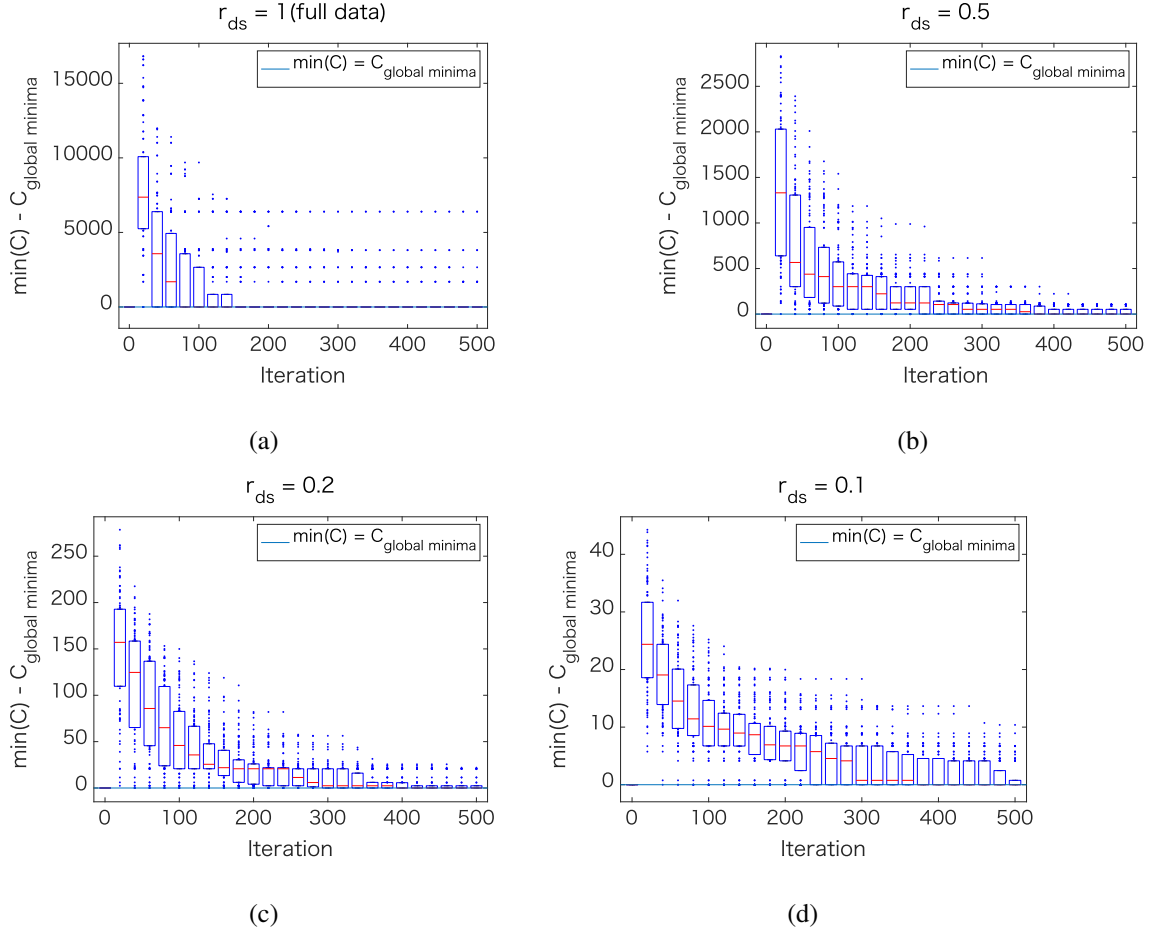


Fig. 5. Performance of BO search in bin width selection for each r_{ds} . The predictive distribution of GP was used to compute the acquisition function. 100 experiments were performed on the same event datasets with different initial $(\Delta_E, \Delta_{qx}, \Delta_{qy}, \Delta_{qz})$ points. The distribution of minimum values of the cost function $\min(C)$ for each experiment is plotted as a function of the iteration number. Here, the baseline is set to the global minimum of the cost function $C_{\text{global minima}}$. Box plotlines show 25th, median, and 75th percentile from the bottom of the box to top. Whisker length is set to 0. Data points outside the boxes are plotted as dots.

4. Discussion

Fig. 4 indicates that the optimal bin widths decrease as the number of data increases, which is in agreement with previous studies.^{14,15,17)} This trend is consistent with Tatsumi et al.'s findings for Cu single crystal, confirming the general applicability of the bin-width optimization theory across different material systems. The optimal bin widths for data down-sampled to 1/5 ($r_{ds} = 0.2$) are comparable with the resolutions determined by experimental conditions such as the sample size and the chopper timing. This implies that the measurement had some redundancy. Therefore, the development of a real-time termination strategy can help to prevent excessive measurement.

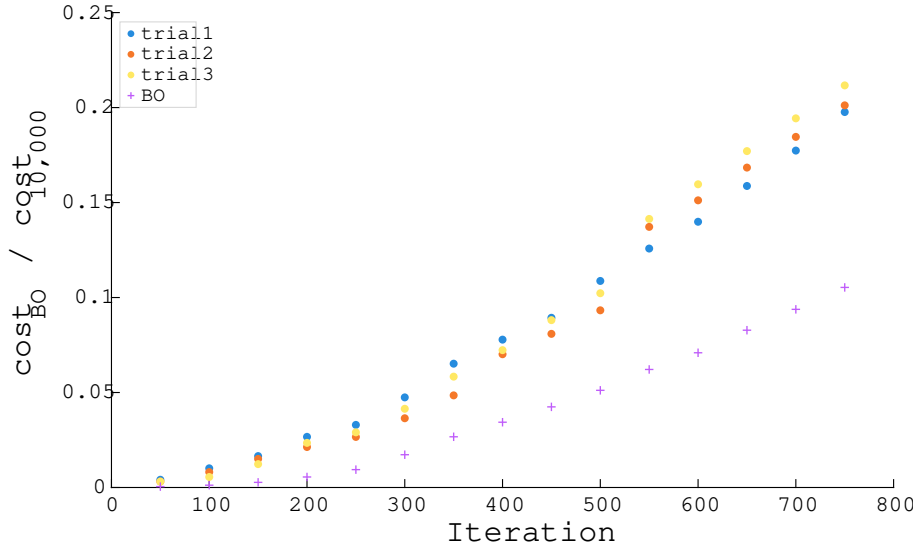


Fig. 6. Comparison of computational costs of the BO search ($cost_{BO}$) with that of an exhaustive search of all 10,000 points ($cost_{10,000}$) for three sample numerical experiments by referring to the sequence of searched points. “BO” represents the computational cost of the acquisition function calculation only. trial 1-3 include both acquisition function computation time and cost function evaluation. At 500 iterations, trial 1, trial 2, and trial 3 reached 10.9%, 9.3%, and 10.2% respectively. It took about 3.9 hours to conduct an exhaustive search of 10,000 points. (CPU: Apple M1 Max; memory: 32 GB).

It is crucial to reduce the computational complexity of the bin-width optimization in the real-time strategy. While Tatsumi et al. achieved real-time optimization by performing a parallel computation on a 32-core Xeon processor,¹⁷⁾ our Bayesian optimization approach could search efficiently without requiring such a parallel infrastructure. Fig. 4 suggests that the landscapes of the cost functions would be smooth. Since GP is effective in interpolating on smooth functions, we expect that BO will work properly. When there was a lot of data, the landscape of the cost function (Fig. 4) around the global minima seemed to be deep. Therefore, BO for bin-width optimization should be satisfactory in cases with a large amount of data. In fact, Fig. 5 shows that BO is especially effective for searching for the optimal bin widths when the number of data is large. Note that we limited the bin-width search space to being a discrete one in this experiment, resulting in $\min(C)$ values in the figure having a discrete structure. In our numerical experiments, it seemed reasonable to set the maximum number of iterations to 500 (Fig. 5). According to Fig. 6, 500 iterations of trial searches cost only about 10% of the exhaustive 10,000 points search. This significant computational cost reduction demonstrates that BO-based bin-width optimization can achieve real-time performance on standard computing environments without parallel infrastructure. Moreover, in “trial2”, the computational

cost significantly increased for iterations between 500 and 550. This was due to an intensive exploration of the small bin-width area.

5. Conclusion

To prevent redundant measurements in inelastic neutron-scattering experiments, we proposed a Bayesian-optimization-based automatic termination strategy for real-time bin-width optimization. The experiment is terminated when the optimal bin widths become smaller than the target resolutions. Through numerical experiments, we demonstrated that this Bayesian optimization can reduce the search cost to approximately 10% of an exhaustive search. By using Bayesian optimization to efficiently search for optimal bin widths, our approach achieves real-time performance without requiring parallel computation infrastructure. Numerical experiments using $\text{Ba}_3\text{Fe}_2\text{O}_5\text{Cl}_2$ data confirmed that optimal bin widths decrease as data accumulates. Even the optimal bin widths for data downsampled to 1/5 were comparable with equipment-limited resolutions, indicating measurement redundancy. This computational efficiency demonstrates that our approach can serve as a practical stopping criterion for routine inelastic neutron-scattering experiments, even on standard single-core computing environments.

Acknowledgment

The authors thank N. Abe, T. Omi, K. Matsuura, K. Ikeuchi, R. Kajimoto, and Y. Inamura for providing us the inelastic neutron-scattering data and the experimental resolutions. This work was partially supported by JSPS KAKENHI Grant-in-Aid for Scientific Research(A) (No. 18H04106), No. JP19H05826, and JST CREST (JPMJCR1761). The inelastic neutron-scattering data of $\text{Ba}_3\text{Fe}_2\text{O}_5\text{Cl}_2$ were obtained by a chopper spectrometer 4SEASONS installed on BL01, J-PARC MLF, Japan, under the proposal No. 2016A0088.

Appendix: Gaussian process

Suppose that we have a training data set \mathcal{D}_n of n observations, $\mathcal{D}_n = \{(\mathbf{x}_i, y_i)\}_{i=1}^n$, where \mathbf{x}_i denotes an input vector of dimension D , and y_i denotes a scalar output. The column input vectors for all n cases are aggregated in the $D \times n$ design matrix $X := (\mathbf{x}_1, \dots, \mathbf{x}_n)$. We assume that each observation is the sum of the objective function f , and independent identically distributed Gaussian noise ϵ

$$y_i = f(\mathbf{x}_i) + \epsilon, \quad (\text{A.1})$$

$$\epsilon \stackrel{i.i.d.}{\sim} \mathcal{N}(0, \sigma^2). \quad (\text{A.2})$$

We assume that the joint distribution of the observations \mathbf{y} and a test output f^* at test input \mathbf{x}^* can be described as

$$\begin{pmatrix} \mathbf{y} \\ f^* \end{pmatrix} \sim \mathcal{N}\left(\mathbf{0}, \begin{bmatrix} K(X, X) + \sigma^2 I & \mathbf{k}(X, \mathbf{x}^*) \\ \mathbf{k}(\mathbf{x}^*, X) & k(\mathbf{x}^*, \mathbf{x}^*) \end{bmatrix}\right). \quad (\text{A}\cdot 3)$$

Here, k denotes a kernel function and $K(X, X)_{i,j} := k(\mathbf{x}_i, \mathbf{x}_j)$. We can analytically calculate the distribution that $f^*|\mathbf{y}$ follows.

$$f^*|\mathbf{y} \sim \mathcal{N}(E[f^*], V[f^*]), \quad (\text{A}\cdot 4)$$

$$E[f^*] = \mathbf{k}(X, \mathbf{x}^*)^T (K(X, X) + \sigma^2 I)^{-1} \mathbf{y}, \quad (\text{A}\cdot 5)$$

$$V[f^*] = k(\mathbf{x}^*, \mathbf{x}^*) - \mathbf{k}(X, \mathbf{x}^*)^T (K(X, X) + \sigma^2 I)^{-1} \mathbf{k}(X, \mathbf{x}^*). \quad (\text{A}\cdot 6)$$

References

- 1) S. W. Lovesey: *Theory of Neutron Scattering from Condensed Matter* (Clarendon Press, Oxford, 1984), Vol. 1.
- 2) J. Thomason: Nuclear Instruments and Methods in Physics Research Section A: Accelerators, Spectrometers, Detectors and Associated Equipment **917** (2019) 61.
- 3) T. Mason, D. Abernathy, I. Anderson, J. Ankner, T. Egami, G. Ehlers, A. Ekkebus, G. Granroth, M. Hagen, K. Herwig, et al.: *Physica B: Condensed Matter* **385** (2006) 955.
- 4) H. Takada, K. Haga, M. Teshigawara, T. Aso, S.-I. Meigo, H. Kogawa, T. Naoe, T. Wakui, M. Ooi, M. Harada, et al.: *Quantum Beam Science* **1** (2017) 8.
- 5) H. Chen, Y. Chen, S. Fu, L. Ma, S. Wang, F. Chen, Y. Chen, H. Dong, L. Dong, G. Feng, et al.: Nuclear Instruments and Methods in Physics Research Section A: Accelerators, Spectrometers, Detectors and Associated Equipment (2025) 170431.
- 6) T. G. Perring, A. D. Taylor, R. Osborn, D. M. Paul, A. T. Boothroyd, and G. Aeppli: Proceedings of the 12th Meeting of the International Collaboration on Advanced Neutron Sources (ICANS-XII), 1994, pp. 1–60. RAL Report 94-025.
- 7) R. I. Bewley, R. S. Eccleston, K. A. McEwen, S. M. Hayden, M. T. Dove, S. M. Bennington, J. R. Treadgold, and R. L. S. Coleman: *Physica B: Condensed Matter* **385–386** (2006) 1029.
- 8) B. Winn, U. Filges, V. O. Garlea, M. Graves-Brook, M. Hagen, C. Jiang, M. Kenzelmann, L. Passell, S. M. Shapiro, X. Tong, et al.: *EPJ Web of Conferences* **83** (2015) 03017.
- 9) D. L. Abernathy, M. B. Stone, M. J. Loguillo, M. S. Lucas, O. Delaire, X. Tang, J. Y. Y. Lin, and B. Fultz: *Review of Scientific Instruments* **83** (2012) 015114.
- 10) R. Kajimoto, M. Nakamura, Y. Inamura, F. Mizuno, K. Nakajima, S. Ohira-Kawamura, T. Yokoo, T. Nakatani, R. Maruyama, K. Soyama, et al.: *Journal of the Physical Society of Japan* **80** (2011) SB025.
- 11) K. Nakajima, S. Ohira-Kawamura, T. Kikuchi, M. Nakamura, R. Kajimoto, Y. Inamura, N. Takahashi, K. Aizawa, K. Suzuya, K. Shibata, et al.: *Journal of the Physical Society of Japan* **80** (2011) SB028.
- 12) S. Itoh, T. Yokoo, S. Satoh, S. Yano, D. Kawana, J. Suzuki, and T. J. Sato: Nuclear Instruments and Methods in Physics Research Section A: Accelerators, Spectrometers, Detectors and Associated Equipment **631** (2011) 90.

- 13) Y. Inamura, T. Nakatani, J. Suzuki, and T. Otomo: *Journal of the Physical Society of Japan* **82** (2013) SA031.
- 14) H. Shimazaki and S. Shinomoto: *Neural Computation* **19** (2007) 1503.
- 15) K. Muto, H. Sakamoto, K. Matsuura, T.-h. Arima, and M. Okada: *Journal of the Physical Society of Japan* **88** (2019) 044002.
- 16) F. C. Crow: *Proceedings of the 11th Annual Conference on Computer Graphics and Interactive Techniques (SIGGRAPH '84)*, 1984, pp. 207–212.
- 17) K. Tatsumi, Y. Inamura, M. Kofu, R. Kiyonagi, and H. Shimazaki: *Applied Crystallography* **55** (2022) 533.
- 18) J. S. Marron and M. P. Wand: *The Annals of Statistics* **20** (1992) 712.
- 19) J. Mockus, V. Tiesis, and A. Zilinskas, The application of Bayesian methods for seeking the extremum, In L. C. W. Dixon and G. P. Szegő (eds), *Towards Global Optimization*, Vol. 2, pp. 117–129. North-Holland, Amsterdam, 1978.
- 20) E. Vazquez and J. Bect: *Journal of Statistical Planning and Inference* **140** (2010) 3088.
- 21) W. Leib and H. K. Müller-Buschbaum: *Zeitschrift für Anorganische und Allgemeine Chemie* **521** (1985) 51.